

Stabilized Kuramoto-Sivashinsky equation: A useful model for secondary instabilities and related dynamics of experimental one-dimensional cellular flows

P. Brunet^{1,2,*}¹*KTH Mechanics, SE 10044 Stockholm, Sweden*²*School of Mathematics, University of Bristol, University Walk, Bristol BS8 1TW, United Kingdom*

(Received 27 March 2006; revised manuscript received 5 June 2007; published 13 July 2007)

We report numerical simulations of one-dimensional cellular solutions of the stabilized Kuramoto-Sivashinsky equation. This equation offers a range of generic behavior in pattern-forming instabilities of moving interfaces, such as a host of secondary instabilities or transition toward disorder. We compare some of these collective behaviors to those observed in experiments. In particular, destabilization scenarios of bifurcated states are studied in a spatially semi-extended situation, which is common in realistic patterns, but has been barely explored so far.

DOI: [10.1103/PhysRevE.76.017204](https://doi.org/10.1103/PhysRevE.76.017204)

PACS number(s): 82.40.Bj, 47.54.-r, 47.20.Ma

An interface that is driven out of equilibrium frequently develops a patterned structure, characterized by a spatially periodic array of identical cells. This pattern can in turn show a set of various secondary instabilities, until a possible transition to disorder [1]. Such a scenario has been encountered in various experiments, such as directional solidification [2,3], directional viscous fingering [4–6], Taylor-Dean flow [7], a locally heated thin layer of liquid [8], or an array of falling liquid columns [9–13].

Coulet and Iooss [14] have proposed a generic model based on broken symmetries which predicts ten secondary instabilities from a primary static periodic cellular structure. This model reproduced successfully many features of secondary modes associated to broken symmetries on the primary pattern; for instance, parity-broken (PB) domains of drifting cells [15] or vacillating-breathing (VB) mode leading to out-of-phase oscillations. However, the model was built under assumptions of slow-varying space-phase variables and thus remained valid only close to secondary thresholds. Gil [16,17] has recently built an extension of this model which includes possible phase mismatch between the primary static state and the bifurcated one. Therefore, Gil's model could reproduce some far-from-secondary-threshold behaviors, such as oscillating patches left behind a propagative domain, black solitons, or spatiotemporal disorder.

Alternative approaches using partial differential equations or cellular automata have been proposed, where the possible dynamical modes are not explicitly introduced in the model, but rather appear via the unstable dynamics of cellular solutions. An example is the stabilized Kuramoto-Sivashinsky (SKS) equation, which is investigated numerically in this paper. In its nonstabilized form, this equation was first built to reproduce some general phenomena in falling film on inclined substrates [18] or in flame-front instabilities [19]. The SKS equation is the following:

$$\frac{\partial f}{\partial t} = -\alpha f + \left(\frac{\partial f}{\partial x}\right)^2 - \frac{\partial^2 f}{\partial x^2} - \frac{\partial^4 f}{\partial x^4}. \quad (1)$$

The term $-\alpha f$ represents the damping term. It has been

shown [20] that this equation was one of the simplest to capture ubiquitous features of pattern-forming instabilities in interfacial growing fronts. This equation is also known to exhibit spatio-temporal intermittency, i.e., co-existence of laminar domains and turbulent patches for a large number of cells [21], while secondary bifurcations have been found as well [20], albeit for a small number of cells (up to 3). However, very few studies focused on secondary instabilities for an intermediate number of cells (typically a few tens). This is the condition under which most experimental interfacial patterns are investigated, and it is expected that collective behaviors with both spatial and temporal significance show up.

In this paper we numerically investigate tertiary bifurcations, i.e., destabilization scenarios on secondary dynamical states. These secondary states are themselves results of the destabilization of a primary static periodic structure. With this semi-constrained (or semi-extended) geometry, the pattern is large enough to show collective behaviors, and small enough to allow for the tracking of the motion and the shape of a single cell. We aim to find a generic comprehensive model for complex states that appear to be due to nontrivial mode coupling or finite-size effects: (i) oscillating wakes behind a propagative domain, (ii) an amplitude hole corresponding to a phase jump in an extended oscillatory state, (iii) oscillations superimposed on a state of drifting cells before its rupture. We show that these tertiary states, among others, can be reproduced by the SKS equation, demonstrating its relevance for phenomena beyond the threshold of secondary instabilities. This paper is divided into two parts: we give a short description of the numerical method, followed by a set of results in the form of spatio-temporal diagrams. Then we comment on similarities and differences with experiments.

a. Results. The resolution of Eq. (1) is carried out by a pseudospectral method. The space derivatives are calculated in Fourier space: multiplication of the vector of the Fourier coefficients, by the vector of the corresponding wave numbers, times the complex imaginary unit i , gives the first space derivative. Any n^{th} space derivative is calculated via the same type of multiplication that is repeated n times. The time derivative of f is then evaluated by a finite difference method. The choice of a small time step (typically around 10^{-3}) is suitable in order to avoid convergence problems. An

*p.brunet@bristol.ac.uk

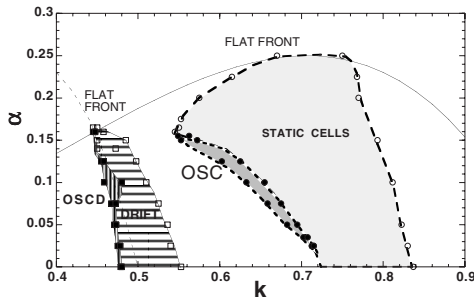


FIG. 1. Stability diagram of the primary and secondary states in the SKS equation. The domains for static cells, oscillating cells (OSC), drifting cells (DRIFT), and oscillating-drifting cells (OSCD), are bounded respectively by open circles, dark circles, open squares, and dark squares. In empty domains, a given state is unstable. The full line stands for the neutral curve of the mode of wave number k , and the dashed line stands for the neutral curve of the mode $2k$.

implicit scheme has been used as well, but is not necessary here: the cellular solutions are smooth enough for a simple explicit scheme to work. We employ periodic boundary conditions and the initial conditions are fixed through the number of cells N_c , using about 25 mesh points per cell.

Inspired by the method employed in [20], we prescribe initial conditions as combinations of sinusoidal functions in order to trigger secondary instabilities from a primary periodic static pattern. Most of the initial conditions consist of a single wave number k plus random perturbations (typical magnitude 1/100). Some states needed specific initial condi-

tions, for example the PB drifting cells, which are obtained from a combination: $f_0(x) = \sin(kx) + a \sin(2kx + \phi_0)$. The phase shift is arbitrarily chosen at 0.5, and the amplitude a is chosen to be equal to 0.5. These two quantities can take values in a certain range (0.3 to 2 for the absolute value of ϕ_0 , 0.25 to 1 for a) without changing the phenomenon qualitatively, but they slightly influence the kinetic properties of the selected states. As the purpose of this study is to seek for destabilization scenarios of secondary bifurcated states, we opt for a set of parameters (k , α , and N_c) such that the system is close to the boundary of existence of the bifurcated states. To compute the temporal evolution of a localized domain of PB cells, we chose the following initial condition: $f_0(x) = \sin(kx \{1 + \frac{a}{2} [1 + \tanh(x_{lim} - x)]\} + a \sin(2kx + \phi_0)) \frac{1}{2} [\tanh(x_{lim} - x) + 1]$. Then between $x=0$ and x_{lim} , the cells are asymmetrical and have a larger wavelength, which corresponds to the domain of stability of drifting cells [20].

Figure 1 gives a cartography of the main states obtained by varying both α and k . The stability of each state is checked by runs of relatively long duration time of one hundred (corresponding to 10^5 time steps): if the state is not broken, it is considered as stable. The symbols stand for the domain boundaries: when these are crossed, the initial state undergoes a transition to another one (sometimes disordered). One of the main reasons for the breakup is the occurrence of the Eckhaus instability [20], which delimitates the domain for static cells. The breakup of drifting states coincides well with the neutral curve of the mode of wavelength $2k$. The oscillating cell (OSC) regime is stable within a much

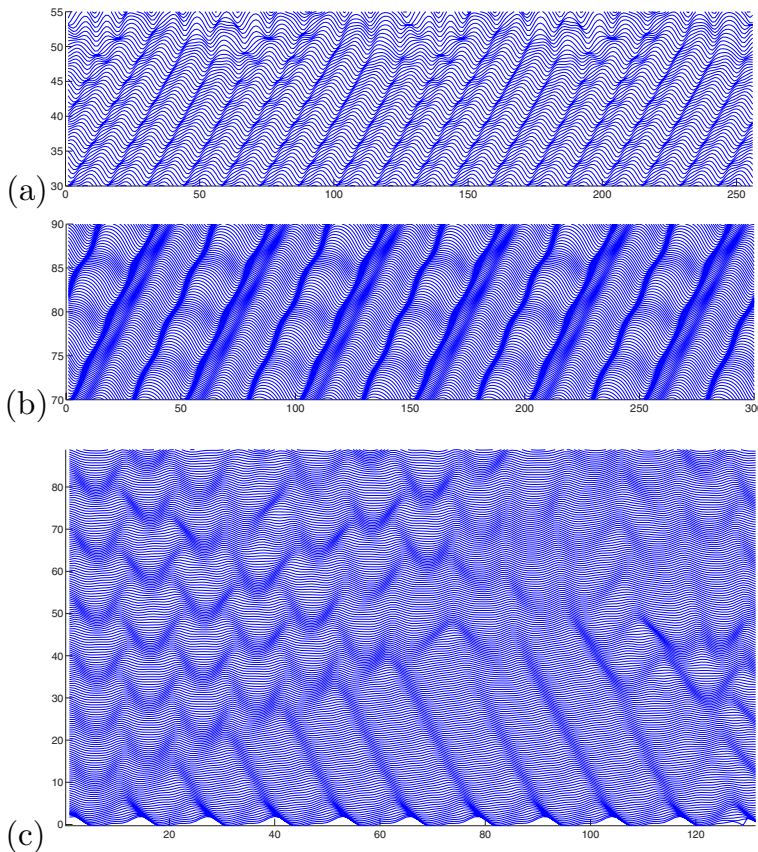


FIG. 2. (Color online) Examples of complex dynamics beyond a secondary instability. (a) A global drift that undergoes in-phase oscillations as a first stage to the breakup towards spatiotemporal disorder ($k=0.47$, $\alpha=0.095$, $N_c=18$). (b) A global drift that undergoes a bifurcation to out-of-phase oscillations ($k=0.53$, $\alpha=0.04$, $N_c=12$). (c) Oscillating wake left behind a domain of drifting cells (extract) ($\alpha=0.15$, $N_c=18$).

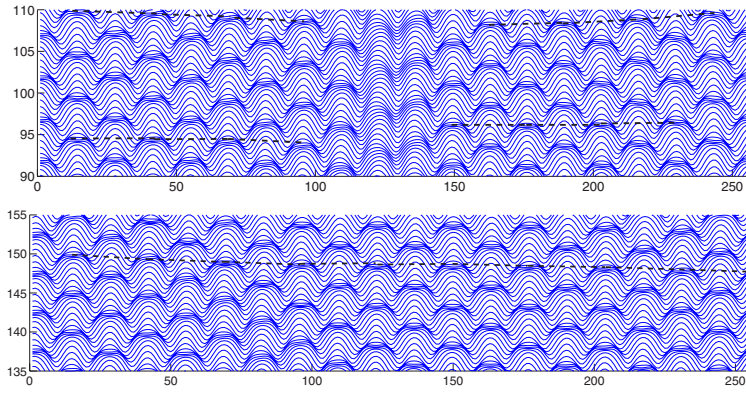


FIG. 3. (Color online) Imperfect extended oscillatory, period-doubling state, caused by an odd number of cells and periodic boundaries. Top: localization of an amplitude hole. Bottom: progressive phase shift. Both obtained with $k=0.64$, $\alpha = 0.1$, $N_c = 19$.

narrower strip than the one predicted by the linear stability analysis [20]. At large α , both drifting and static states undergo a transition to a flat front and the cellular pattern vanishes: it corresponds to the neutral curve of the mode k .

Typical spatiotemporal diagrams are depicted on Fig. 2, and reproduce complex collective behaviors (a)–(c) reminiscent of various experiments of patterned interfaces. Time runs vertically from bottom to top. These diagrams are obtained by plotting $f(x, t)$ every n^{th} time step, added to a vertical shift proportional to the value of time. The case (a) represents a state of drifting cells, initially traveling at constant speed, which undergoes an oscillatory instability in a second step, to ultimately break up and enter a disordered regime. The case (b) is similar to (a), except that each cell oscillates out of phase of its nearest neighbors. These oscillations are likely to become amplified and lead to spatiotemporal disorder, such as in case (a). Case (c) shows a local domain of drifting cells, propagating opposites of drift, and leaving oscillatory patches behind its trailing edge.

A second kind of behavior concerns phase imperfections

in extended oscillatory regimes, Fig. 3. These diagrams are obtained when an oscillatory state develops and exhibits a so-called “optical mode” (by analogy to eigenmodes in phonons), i.e., neighbor cells oscillating out of phase. While such a state can be almost perfectly homogeneous if the number of columns is even, it will necessarily adapt to a nonhomogeneous spatial phase for an odd number of columns. These diagrams show that the phase imperfection can be twofold: it can either be sharply localized (top diagram in Fig. 3) or evenly dispatched on the pattern (bottom diagram). In this second case, the dashed line describes the isophase of the double-period state. The first case exhibits an amplitude hole, i.e., the amplitude of oscillations vanishes in the vicinity of the phase imperfection, enabling the pattern to have a sharp phase jump of π .

b. Discussion: Comparisons with experiments. We now argue that the features depicted above reproduce destabilization scenarios observed in several experiments. We start with a presentation of quantitative data on the PB drifting cells. Figure 4 shows general trends of the drift speed V_d , mea-

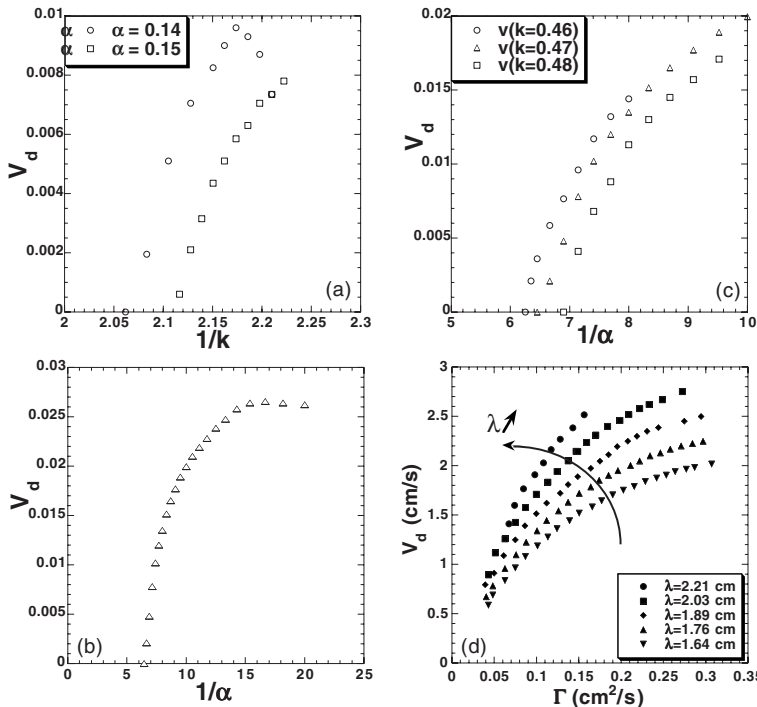


FIG. 4. Measurements of drifting velocities in the SKS equation (a),(b),(c) and in the experimental pattern of liquid jets (d). (a) Versus $1/k$ for two values of α . (b) Versus $1/\alpha$ for $k=0.47$. (c) Versus $1/\alpha$ for various k (close up around threshold). (d) Drift velocities versus flow rate, for different wavelengths (silicon oil of viscosity $\eta=100$ cP).

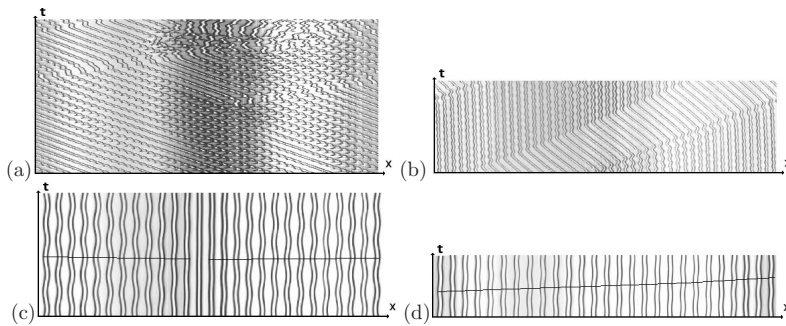


FIG. 5. Various collective behaviors in the pattern of liquid columns (viscosity $\eta=100$ cP), reproduced by the SKS equation. (a) Oscillations superimposed on a state of global drifting cells, leading ultimately to disorder. (b) An oscillating wake in the trailing edge of a propagating domain. (c) A phase defect localized in an oscillatory state. (d) Progressive phase shift in an oscillatory state.

sured on a globally extended drifting state in both the SKS equation (a)–(c) and a pattern of falling jets (d) [10,13]. The distance along x is chosen such as the length of a cell equals one. Figure 4(a) shows the dependency of V_d versus $1/k$, for two values of α . Figures 4(b) and 4(c) show V_d versus $1/\alpha$: the general trend is a sharp increase of the speed just above a threshold value for α . Let us also recall that the drift velocity of PB cells in the pattern of columns (V_d) increases as the square root of Γ (the flow rate per unit length), see Fig. 4(d). If one tries to get a similar relationship for the SKS equation, it turns out that identifying the control parameter with $1/\alpha$, is the most relevant choice [compare Figs. 4(b), 4(c), and 4(d)]. In the pattern of columns, a similar dependance on k was found: the drift speed increases with $1/k$ for most of the conditions [Fig. 4(a)]. In other experiments, the identification of $1/\alpha$ with the control parameter of the PB bifurcation is also straightforward: in the printer's instability, it is the rotation speed of the internal cylinder [6] and in directional solidification it is a combination of the wavelength λ and the pulling velocity V that reads: λV^2 .

The dynamics depicted in Fig. 2 are commonly observed in experiments. Case (a) is reminiscent of various experiments [3,7,13]. It can either appear under temporal modulations of the control parameter [7] or simply when the control parameter is increased sufficiently beyond the threshold of drifting cells [3,13]. Case (b) has only been observed in directional solidification and referred to as T- 2λ O in [3]. Case (c) is observed in both directional viscous fingering [5] and an array of liquid columns [11,13]. It shows the link between the parity-breaking and vacillating-breathing modes: in this case the relaxation at the rear wall of the propagative dilation wave (drifting cells are dilated compared to static cells) leads to oscillations at the trailing edge of the domain. These os-

cillations are the local counterparts of the ones in Fig. 3. Two of these destabilizing behaviors are reproduced on Figs. 5(a) and 5(b) for the pattern of liquid columns [11,13].

We now examine the phase imperfections in an oscillatory state (Fig. 3). The two types of phase imperfections on an extended oscillating state have been observed in the pattern of columns [13] for an odd number of columns (whereas an almost homogeneous oscillatory state is observed for an even number of columns), as shown on Figs. 5(c) and 5(d). It should be noted, however, that the SKS equation failed to reproduce a sustained propagating domain of PB cells. Such a domain is bound to shrink and to vanish after a while, at least in the explored parameter range. Thus probably, a state of PB cells remains stable only for an extended drifting state.

In conclusion, the presented results show that the SKS equation is able to reproduce a set of complex situations that occur for some secondary instabilities of pattern-forming experiments. We have chosen a semi-extended pattern (a few tens of cells), as this is frequently encountered in experiments, and we have taken parameters and initial conditions in order to trigger further destabilization of secondary bifurcated states. The fact that such realistic behaviors are reproduced by a simple generic equation such as (1), provides an interesting perspective for studying tertiary bifurcations. This includes a disordered regime with occurrences of phase defects [such defects appear on top of diagram Fig. 2(a)], already reported in [20] for a small number of cells and also obtained for a larger number of cells (a few tens) in our simulations. A comprehensive study of such a regime based on statistics of defect occurrences, would be of great interest.

J. Hoepffner and L. Brandt are kindly acknowledged for their help in building the code. We thank J.H. Snoeijer for a critical reading of the manuscript.

- [1] M. C. Cross and P. C. Hohenberg, *Rev. Mod. Phys.* **65**, 851 (1993).
- [2] J.-M. Flesselles *et al.*, *Adv. Phys.* **40**, 1 (1991).
- [3] M. Ginibre *et al.*, *Phys. Rev. E* **56**, 780 (1997).
- [4] M. Rabaud *et al.*, *Phys. Rev. Lett.* **64**, 184 (1990).
- [5] S. Michalland and M. Rabaud, *Physica D* **61**, 197 (1992).
- [6] L. Pan and J. R. de Bruyn, *Phys. Rev. Lett.* **70**, 1791 (1993).
- [7] S. G. K. Tennakoon *et al.*, *Phys. Rev. E* **54**, 5053 (1996).
- [8] J. Burguete *et al.*, *Physica D* **174**, 56 (2003).
- [9] C. Counillon *et al.*, *Phys. Rev. Lett.* **80**, 2117 (1998).
- [10] P. Brunet *et al.*, *Europhys. Lett.* **56**, 221 (2001).
- [11] P. Brunet *et al.*, *Eur. Phys. J. B* **35**, 525 (2003).
- [12] P. Brunet and L. Limat, *Phys. Rev. E* **70**, 046207 (2004).
- [13] P. Brunet *et al.*, *Eur. Phys. J. B* **55**, 297 (2007).
- [14] P. Couillet and G. Iooss, *Phys. Rev. Lett.* **64**, 866 (1990).
- [15] R. E. Goldstein *et al.*, *Phys. Rev. A* **43**, 6700 (1991).
- [16] L. Gil, *Europhys. Lett.* **48**, 156 (1999).
- [17] L. Gil, *Physica D* **147**, 300 (2000).
- [18] Y. Kuramoto, *Chemical Oscillations, Waves and Turbulence* (Springer-Verlag, Berlin, 1978).
- [19] G. I. Sivashinsky, *Acta Astronaut.* **4**, 1177 (1977).
- [20] C. Misbah and A. Valance, *Phys. Rev. E* **49**, 166 (1994).
- [21] H. Chaté and P. Manneville, *Phys. Rev. Lett.* **58**, 112 (1987).
- [22] K. R. Elder *et al.*, *Phys. Rev. E* **56**, 1631 (1997).